Pediatr Radiol (2012) 42:1089–1098
DOI 10.1007/s00247-012-2423-1

ORIGINAL ARTICLE

A prospective study of radiographic manifestations in Hutchinson-Gilford progeria syndrome

Robert H. Cleveland · Leslie B. Gordon · Monica E. Kleinman · David T. Miller · Catherine M. Gordon · Brian D. Snyder · Ara Nazarian · Anita Giobbie-Hurder · Donna Neuberg · Mark W. Kieran

Received: 23 February 2012 / Revised: 6 April 2012 / Accepted: 23 April 2012 / Published online: 1 July 2012

Abstract
Background Progeria is a rare segmental premature aging disease with significant skeletal abnormalities. Defining the full scope of radiologic abnormalities requires examination of a large proportion of the world's progeria population (estimated at 1 in 4 million). There has been no comprehensive prospective study describing the skeletal abnormalities associated with progeria.
Objective To define characteristic radiographic features of this syndrome.
Materials and methods Thirty-nine children with classic progeria, ages 2–17 years, from 29 countries were studied at a single site. Comprehensive radiographic imaging studies were performed.
Results Sample included 23 girls and 16 boys—the largest number of patients with progeria evaluated prospectively to date. Eight new and two little known progeria-associated radiologic findings were identified (frequencies of 3–36%). Additionally, 23 commonly reported findings were evaluated. Of these, 2 were not encountered and 21 were present and

L.B.G. is the parent of a child with HGPS who participated in this study.

R. H. Cleveland (✉)
Department of Radiology, Children's Hospital Boston,
Harvard Medical School,
300 Longwood Avenue,
Boston, MA 02115, USA
e-mail: robert.cleveland@childrens.harvard.edu

L. B. Gordon · M. E. Kleinman
Department of Anesthesia, Children's Hospital Boston,
Harvard Medical School,
Boston, MA, USA

L. B. Gordon
Department of Pediatrics, Hasbro Children's Hospital,
Warren Alpert Medical School of Brown University,
Providence, RI, USA

D. T. Miller
Division of Genetics, Children's Hospital Boston,
Harvard Medical School,
Boston, MA, USA

C. M. Gordon
Division of Endocrinology and Adolescent Medicine,
Children's Hospital Boston, Harvard Medical School,
Boston, MA, USA

B. D. Snyder
Department of Orthopedic Surgery, Children's Hospital Boston,
Harvard Medical School,
Boston, MA, USA

A. Nazarian
Harvard Medical School,
Boston, MA, USA

A. Giobbie-Hurder · D. Neuberg
Department of Biostatistics and Computational Biology,
Dana-Farber Cancer Institute,
Boston, MA, USA

D. Neuberg
Department of Biostatistics, Harvard School of Public Health,
Boston, MA, USA

M. W. Kieran
Division of Pediatric Oncology, Dana-Farber Cancer Institute
and Children's Hospital Boston,
Boston, MA, USA

ranked according to their frequency. Nine abnormalities were associated with increasing patient age (P=0.02–0.0001).
Conclusion This study considerably expands the radiographic morphological spectrum of progeria. A better understanding of the radiologic abnormalities associated with progeria and improved understanding of the biology of progerin (the molecule responsible for this disease), will improve our ability to treat the spectrum of bony abnormalities.

Keywords Progeria · Phenotype · Skeletal findings · Frequency · Children

Introduction

Hutchinson-Gilford progeria syndrome (HGPS or progeria) is a sporadic, rare autosomal-dominant disorder that presents as a segmental model of premature aging affecting multiple organ systems. The classic progeria mutation is a de novo heterozygous c.1824C>T base substitution within the *LMNA* gene, located on chromosome 1q [1, 2]. The *LMNA* gene normally encodes the inner nuclear membrane protein, lamin A, serving both structural and regulatory functions in most cell types [3]. The silent mutation creates a cryptic splice site, resulting in a shortened and aberrant protein product called progerin [2]. The cellular defects in progeria stem from accumulation of progerin leading to nuclear membrane distortion and a decreased cellular lifespan [4, 5]. Clinical manifestations likely stem from accumulation of progerin within tissues [6, 7] and abnormal transcription of hundreds of genes that lie downstream of the *LMNA* defect [8–10].

HGPS was first identified nearly 126 years ago, with a single case report by Sir Jonathan Hutchinson in 1886, and was further described by his colleague Hastings Gilford in a series of case reports starting in 1897 in which he coined the term “progeria” to describe the syndrome. In 1928, an article in French by Waldorp and del Castillo used the conjoined eponym "Hutchinson-Gilford syndrome" for the first time [11]. Gene mutation identification came nearly 117 years later in 2003 [1, 2].

Patients with the classic gene mutation for HGPS have a normal appearance at birth. By 1 year of age, there is progressive development of characteristic signs and symptoms [12]. These include generalized growth failure, alopecia, significant loss of subcutaneous fat, joint contractures and extreme short stature, along with multiple additional features. Later in childhood, atherosclerosis is apparent and children die of myocardial infarction or cerebral vascular accidents at an average age of 13 years [11].

Skeletal involvement results in a characteristic facial appearance with retrognathia, crowded dentition, narrowed nasal bridge, as well as short stature. The largest retrospective skeletal survey of patients with HGPS evaluated by conventional radiography reported osteopenia, narrowed bones with accentuated demineralization at the ends of long bones comprising the appendicular skeleton, coxa valga, hip dysplasia, avascular necrosis, acro-osteolysis, narrow chest apices, small clavicles, resorption of the distal clavicles, thin ribs, resorption of the anterior ribs, rib fractures, ovoid vertebral bodies, cardiomegaly, diastasis of the cranial sutures and Wormian bones [13]. Others have noted kyphoscoliosis [14, 15]. Recently, using peripheral quantitative CT (pQCT) and dual-energy x-ray analysis (DXA), we demonstrated in a subgroup of the cohort of HGPS patients investigated here that the bone structure of the appendicular skeleton was highly dysmorphic [16]. Analysis of DXA data indicated that these children had moderately low Z-scores for the projected area bone mineral density (aBMD) at the lumbar spine and proximal femur, which improved after adjustment for height age, while the overall actual volumetric BMD measured at the radius using pQCT was not different for children with HGPS compared to normal age-matched controls. Further cross-sectional pQCT images revealed distinct abnormalities of the structural geometry at the diaphysis and metaphysis of the radius in children with HGPS compared with healthy controls. Taken together, these findings suggested that the phenotype of HGPS represents a unique skeletal dysplasia.

The objective of the current study was to provide a comprehensive survey of the skeletal dysmorphisms observed in children with HGPS using conventional radiography. We identified radiographic findings from 39 children with the classic HGPS genotype, representing approximately 15–20% of the world’s HGPS population—the largest number of children with this syndrome to be reviewed prospectively. To date, only one prospective study has reported a limited set of radiographic findings for children with HGPS [17]. The results of this current study add information for characterizing the skeletal abnormalities associated with HGPS and provide reliable data on which to base treatment study outcomes.

Materials and methods

Study population

Participants were flown to the central study site, from 29 countries speaking 14 languages. Ages ranged from 2.2 years to 17.5 years. There were 23 boys and 16 girls. All had the classic clinical phenotype and a genetically confirmed *LMNA* c.1824C>T (p.Gly608Gly) mutation [12]. Most pre-trial clinical information was obtained from the Progeria Research Foundation Medical and Research

Database (Brown University Center for Gerontology and Healthcare Research, Providence, RI) with parental consent. For some patients, pre-trial clinical information was provided directly from the referring physicians.

Children were enrolled into either of two clinical trials for progeria (see study numbers NCT00425607 and NCT00916747, http://clinicaltrials.gov/). As such, the children included in this present study are included in databases providing information for other investigations, including one published earlier [16]. However, the conventional imaging characteristics have not previously been categorized or reported. Only the baseline, pre-treatment X-ray studies are reported in this study. They have not been reported elsewhere.

Consent and oversight

The central study site's Committee on Clinical Investigation approved both study protocols. Written informed consent was obtained from the parents of all participants and study assent was obtained from children old enough to partake in the consent process. Consent was provided in written and oral form in the language of the parents and interpreters were provided during all testing periods for non-English-speaking participants. The study was HIPAA-compliant and overseen by a data and safety monitoring committee.

Radiographic imaging

Images included AP of the hands, PA and lateral of the chest, AP and frog views of the pelvis (n=39) with dental images including an AP of much of the skull (n=30). Subsequently, AP and lateral images of each humerus, forearm and lower leg were added to the protocol. A subgroup of the 39 children received these additional images (n=13). All images were interpreted by the lead author (R.H.C.), an American Board of Radiology subspecialty-certified pediatric radiologist with 36 years' experience.

Statistical analyses

Comparisons of age-related incidences of observations were performed using Fisher exact test with statistical significance defined as a two-sided $P \leq 0.05$.

Results

Thirty-one skeletal abnormalities were detected on radiographic images. Table 1 lists the observations and the number and percentage of children who exhibited the observation in descending order of frequency. Eight of these observations have not previously been reported as associated with HGPS. Two have been rarely mentioned as associated with HGPS. These ten observations are shown in Figs. 1, 2, 3 and 4. Those findings with age specificity are listed in Table 2.

Of the eight newly recognized observations, a focal concave cortical defect at or near to the insertion of a major muscle group was the most common, seen in 14 of 39 (36%) children at one or multiple sites. In the nine children with imaging of the forearm and lower leg, it was present in the proximal ulnar aspect of the radius (insertion of biceps) in seven and in the proximal tibial metadiaphysis (below the insertion of the patella tendon) in five (Fig. 1). It was noted to affect the lateral aspect of the femoral greater trochanter (insertion of gluteus medius) in four children, the medial femoral neck (above the insertion of iliopsoas; MRI in one child shows this to be at the attachment of the joint capsule) in five children and the proximal humerus (insertion of deltoid) in one child (Fig. 1). Of the 14 affected children, 9 had the defect at 1 site, 3 children were affected at 2 sites, and 2 children were affected at 4 sites. When present, these defects were often but not universally bilateral. In one child, there was questionable internal partial ossification. Younger children with minimal or no ossification of the femoral greater trochanter did not exhibit focal cortical concave defects at that site (Table 2).

Dystrophic calcifications have rarely been reported in HGPS [18] but were present in 11 of the 39 (28%) children (Fig. 2). Several children had these abnormal calcifications in multiple sites. However, the most common site was distal to the tufts of the fingers (7/11). Particularly at that site, the calcifications were often popcorn-like (Fig. 2) and similar to those seen with dermatomyositis, scleroderma and thermal injury [19].

Growth disturbances of the distal radius and ulna were seen in 38% (15/39) of the children: mild instances of ulnar minus wrist deformity were present in 12 of 39 (31%) children and Madelung-like deformity was present in 3 of 39 (8%) (Fig. 3). Enlargement of the proximal femur (coxa magna) (10/39, 26%) (Fig. 1) and humerus (5/39, 13%) (Fig. 4) has been reported previously [13]. However, in children in whom the distal femur and distal humerus were imaged (9/39), comparable enlargement of the distal long bones was consistently present when proximal enlargement was noted (Fig. 4). An unusual elongation and overgrowth of the femoral greater trochanter was present in 9/39 children (23%) (Figs. 1 and 5).

Pseudoarthrosis of one or both distal clavicles has rarely been reported with HGPS [20] but was present in 9/39 children (23%) (Fig. 6).

Three findings were observed in one child and are recognized as normal variants and are not likely associated with HGPS. There were bifid ribs and congenitally fused ribs

Table 1 Rank order of observations

Observation	Children affected (n=39)	% Affected
Small clavicles	39	100
Coxa valga	37	95
Acroosteolysis	36	92
Resorption of the distal clavicles	32	82
Narrow apices	32	82
Hip dysplasia	27	69
Thin ribs	23	59
Resorption of the anterior ribs	17	44
Closed sagittal suture	13 (n=30)[e]	43
Generalized osteopenia	15	38
Focal cortical defect[a]	14[f]	36
Flexed fingers	14	36
Ulnar minus variant[a]	12	31
Enlarged heart	12	31
Dystrophic calcification[b]	11	28
Sagittal suture diastasis	8 (n=30)[e]	27
Enlarged femoral head[c]	10	26
Pseudoarthrosis[b]	9	23
Enlarged femoral greater trochanter[a]	9	23
Avascular necrosis of the proximal femur	7	18
Kyphoscoliosis	6	15
Enlarged humoral head[c]	5	13
Narrowed humoral diaphysis	5	13
Prominent pulmonary vessels	5	13
Wormian bones	4 (n=35)[e]	11
Accentuated osteopenia of proximal humoral/femoral epiphysis	4	10
Rib fracture	4	10
Madelung deformity[a]	3	8
Ivory epiphyses[a]	1	3
Bifid rib[a]	1	3
Congenitally fused ribs[a]	1	3
Narrowed femoral diaphysis[d]	0[g]	0
Oval vertebrae[d]	0	0

[a]New observation

[b]Observation rarely noted in Hutchinson-Gilford progeria syndrome (HGPS)

[c]When femoral and humeral heads were enlarged and the distal aspect of the long bone was imaged, it was always comparably enlarged. The distal enlargement is a newly noted observation (the distal femur and humerus were only imaged in 9 of the children)

[d]Previously published findings that we did not observe

[e]Imaging did not provide adequate assessment for this observation in some of the children accounting for the n of less than 39

[f]Focal cortical defects were noted in the metadiaphyses of multiple long bones in 11 children and in the greater trochanter of the femur in 4 children. Five children had these in multiple bones

[g]The femoral diaphysis was not completely imaged in these children, therefore this observation is inconclusive

(seen in the same child) [21], as well as ivory epiphyses [22].

Two observations previously associated with progeria were not observed in the present cohort. These were oval vertebrae [14, 15] and narrowed femoral diaphyses [14]. However, the femoral diaphyses were not specifically imaged in this study and therefore the observation of narrowing might have been unapparent.

Many of the classic manifestations of progeria were confirmed [14]. These observations are typically reported in survey textbooks of syndromes and other dysmorphic conditions. For ease of reader access and comprehensive listing of observations, references to these classic manifestations will be to these textbooks.

Skull Sagittal suture diastasis was present in 8/30 (27%). However, with maturation of the children the sagittal suture assumed a normal configuration. This is not unexpected as the cranial sutures narrow and close with advancing age. The oldest child with sagittal suture diastasis was 7.2 years. The earliest age at which the sagittal suture was closed was 2.5 years with mean age of closure of 8.8 years. Wormian bones were present in 4/35 patients (11%).

Chest Narrow chest apices were present in 32/39 (82%). Small clavicles were found in 39/39 (100%), resorption of the distal clavicles in 32/39 (82%), thin ribs in 23/39 (59%) and resorption of the anterior ribs in 17/39 (44%). Rib fractures were present in 4/39 children

Fig. 1 Cortical notch defect. **a** Radiograph in a 5-year-old girl with progeria and a cortical notch defect. Cortical notch defects when present in the radius were always situated in the proximal diaphysis along the ulnar aspect, essentially at the site of the radial tuberosity (*arrow*). **b** Radiograph in a 10-year-old girl with progeria and a cortical notch defect. When present in the tibia, the cortical notch defects were in the anterior cortex of the proximal diaphysis somewhat below the level of the normal concavity associated with the tibial tubercle apophysis (*arrow* tibial tubercle; *arrowhead* abnormal cortical notch). **c** Radiograph in a 5-year-old girl with progeria and a cortical notch defect. The defect was always similarly placed in the anterior proximal diaphyseal cortex when present in the tibia (*arrow*). **d** Hip radiograph in a 9-year-old boy with progeria and a cortical notch defect. When the greater trochanter was enlarged and elongated, it often had a laterally placed notch defect (*arrows*). (Also note the presence of hip dysplasia, coxa valga and moderately enlarged proximal femurs.) **e** Hip radiograph in a 5-year-old girl with progeria and a cortical notch defect. When present in the femoral neck, cortical notch defects were situated in the mid aspect of the medial margin, as noted on the left in this child (*arrow*). (Also note the presence of hip dysplasia, coxa valga and moderately enlarged proximal femurs.) **f** Radiograph in a 10-year-old girl with progeria and a cortical notch defect in the proximal anterior diaphysis of the right humerus (*arrow*). There is questionable partial internal ossification

(10%). Heart size was judged as enlarged in 12/39 children (31%) and the pulmonary vasculature as prominent in 5/39 children (13%).

Scoliosis Kyphoscoliosis has been reported [14]. The extent of convexity of the spinal deformity (expressed in degrees of the subtended arc) in frontal plane deformity (scoliosis) and in the sagittal plane (kyphosis) was assessed using the Cobb method [23]. A scoliosis of the thoracolumbar spine (defined as the presence of a mild undulating curve, $n=3$: major curves of 7, 12 and 13 degrees) or a Cobb angle of 15 degrees or greater ($n=2$: 16 and 18 degrees) and/or a kyphosis (defined as a Cobb angle of 45 degrees or greater, $n=3$: 57, 68, and 83 degrees) was present in 6/39 children (15%). Two of the children with a scoliosis greater than 15 degrees also had a kyphosis of greater than 45 degrees.

Hip Several observations pertaining to the hips seem to be integral to the progeria phenotype (Figs. 1 and 5). Coxa valga [14] was present in 37/39 (95%), hip dysplasia in 27/39 children (69%), an enlarged proximal femur (coxa magna) [13] in 10/39 (26%), an enlarged elongated femoral greater trochanter in 9/39 (23%) and avascular necrosis (AVN) [14] of the proximal femur in 7/39 (18%).

Humerus A similar alteration in long bone morphology was also recognized in the proximal humerus. The humeral head was enlarged [7] in 5/39 (13%) and the diaphysis was

Fig. 2 Dystrophic calcifications. **a** Leg radiograph in a 17-year-old boy with progeria and dystrophic calcifications. Dystrophic soft-tissue calcifications were seen over the chest, abdomen and extremities. They were often linear, curvilinear or clumped (as in this child's lower leg) (*arrow*). **b** Radiograph in a 3-year-old girl with progeria and dystrophic calcifications. When calcifications were adjacent to the digital tufts, they frequently were popcorn-like in their configuration as seen in the second digit. (Also note variable degrees of acroosteolysis of the tufts)

narrowed [14] in 5/39 (13%) (Fig. 4). Only enlargement of the proximal humerus and femur has been reported [13]. However, in the current study, in those instances where both ends of the bone were imaged, if the proximal end of the long bone was enlarged, the distal metaphysis and epiphysis were comparably enlarged (Fig. 4). In every child in whom enlargement of both the ends of the humerus was noted, there was comparable enlargement of both the ends of the femur. There were five children with mild enlargement of the ends of the femur in whom the ends of the humerus were not notably enlarged.

Hand Acroosteolysis of phalangeal tufts was present in 36/39 (92%) (Fig. 3). Flexion of the fingers associated with the generalized flexion contractures that occur in progeria [17] was present on bone age images of 14/39 (36%). Bone age estimates were performed using the standards of Greulich and Pyle [24]: 18/39 (46%) were within 1 standard deviation (SD) of the norm, 11/39 (28%) were within 2 SD of the norm, 6/39 (15%) were within 3 SD above the norm, 1/39 (3%) was within 3 SD below the norm, 3/39 (8%) were 3 or more SD above the norm and none was 3 or more SD below the norm.

Osteopenia Generalized osteopenia was judged as present in 15/39 children (38%) and accentuated osteopenia as present at the proximal humerus and or femur in 4/39 patients (10%).

Because HGPS is a progressive disease that can exhibit age-associated bone abnormalities [13], we compared abnormalities between younger and older age groups. Consequently the children were divided into two groups of approximately equal size based on age at initial imaging; 18 patients ages 2–5 years (39% male) and 21 ages 6–18 years (38% male). Table 2 lists eight skeletal findings that were significantly more common in the older patient

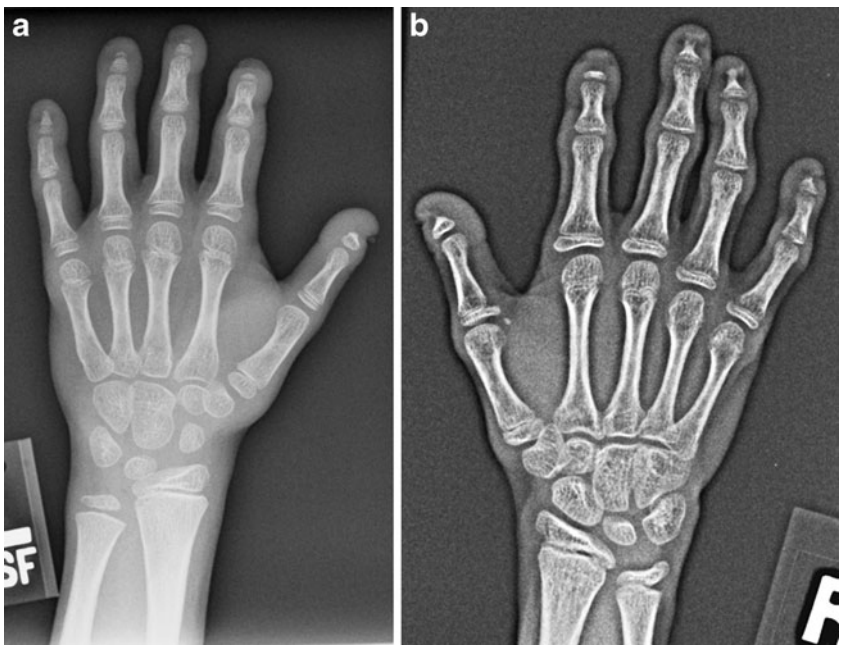

Fig. 3 Ulnar minus variant. **a** In this radiograph in an 8-year-old boy with progeria there is relative foreshortening of the ulna consistent with mild ulnar minus variant. (Also note variable degrees of acroosteolysis of the tufts.) **b** Radiograph in a 10-year-old girl with progeria with Madelung-like deformity. There is a mildly angular contour formed by the distal radius and ulna, with the median aspects of each sloping proximally, consistent with a mild Madelung-like deformity. Also note variable degrees of acroosteolysis of the tufts and dystrophic calcifications distal to several of the tufts

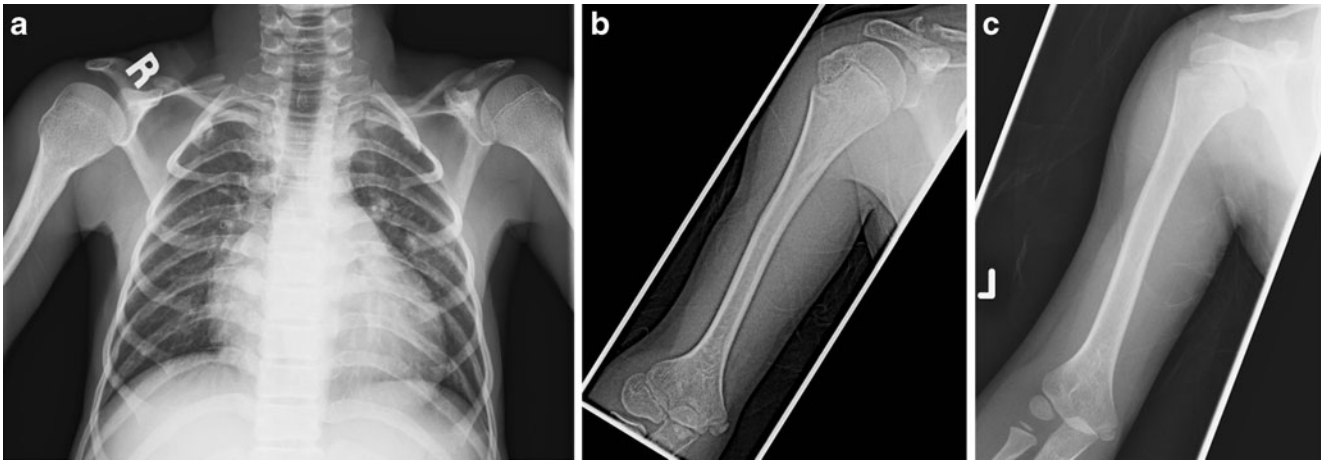

Fig. 4 Enlarged proximal and distal humerus. **a** In this chest radiograph of a 17-year-old boy with progeria the proximal humerus is moderately enlarged bilaterally. (Also note narrow pulmonary apices, small clavicles with distal resorption, thin ribs with anterior resorption and cardiomegaly.) **b** This upper arm radiograph in a 12-year-old boy with progeria shows mild enlargement of the proximal humerus with comparable enlargement of the distal humerus, particularly laterally. The diaphysis is mildly narrowed. (Also note pseudoarthrosis of the distal clavicle.) **c** Radiograph of a 4-year-old sister of the boy in image **b**, who also has progeria; this image reveals normal-size proximal and distal humerus without diaphyseal narrowing. (Also note mild resorption of the distal clavicle, which is mildly narrowed)

group, and one that was more common in the younger patient group.

Discussion

The objective of this study was to provide a comprehensive survey of the skeletal dysmorphisms observed in patients with HGPS evaluated using conventional radiography. This study presents the only prospective radiographic examination of approximately 15–20% of the world's HGPS population, encompassing significant gender, age and ethnic diversity. The only other prospective study of children with HGPS was relatively limited and identified only acroosteolysis, clavicular resorption and coxa valga in all 15 of its subjects [17]. This current study extends the previous retrospective radiographic study of HGPS [13] by identifying new HGPS-related skeletal dysmorphisms and findings that are apparently age-related. These observations might allow us to examine more closely the root causes of the skeletal abnormalities associated with HGPS. In addition, as children of all ages with HGPS undergo new treatment trials initiated at all ages, we can closely follow the progression, regression or delayed onset of skeletal abnormalities in response to the therapies. Only a sufficiently large and uniformly studied baseline cohort can yield these types of treatment analyses.

Of the eight newly recognized observations, a focal concave cortical defect at or near to the insertion of a major muscle group was the most common, seen in 14/39 children (36%). Although many of the defects are at the insertion of muscles, some are merely relatively close to an insertion site. Whether the defects relate to abnormal tension, are a component of a skeletal dysplasia or are an unrecognized abnormality of mesodermal proliferation is unknown.

Table 2 Age-related observations

Observation[a]	2–5 years (%)[b]	6–18 years (%)	*P*-value
Thin ribs	4/18 (22%)	19/21 (90%)	<0.0001
Resorption of the anterior ribs	2/18 (11%)	15/21 (71%)	0.0003
Generalized osteopenia	2/18 (11%)	11/19 (58%)	0.005
Flexed fingers	1/18 (6%)	13/21 (62%)	0.0003
Ulnar minus variant	2/18 (11%)	10/21 (48%)	0.02
Sagittal suture diastasis[c]	6/11 (55%)	2/19 (11%)	0.03
Enlarged femoral head	3/18 (17%)	11/19 (58%)	0.02
Pseudoarthrosis	0/18 (0%)	9/21 (43%)	0.002
Enlarged femoral greater trochanter	1/18 (6%)	8/21 (38%)	0.02

[a]Rates are indicated only for those observations with a statistical difference between age groups

[b]Incidences are reported as the percentage (%) of children within each age group with the presence of the observation

[c]This is not unexpected as the cranial sutures narrow and close with advancing age

Fig. 5 Hip radiograph in a 10-year-old girl with progeria with enlarged irregular-shape greater trochanter. Once the femoral greater trochanter begins to calcify, it often becomes enlarged and elongated superiorly. Also note small cortical notch defects in both medial femoral necks, left more pronounced than the right (*arrows*). There is mild hip dysplasia, with coxa valga and moderately enlarged proximal femurs (coxa magna)

Dystrophic calcifications, previously rarely recognized as a component of HGPS, were present in 11/39 (28%) children. The precise etiology of these calcifications is unclear but might relate to microvascular compromise as suggested in dermatomyositis, scleroderma and thermal injury [19, 25–27].

Ulnar minus variant [28] and Madelung deformity [29]—both abnormalities of the distal radius and/or ulna—have been reported with various syndromes [30, 31] and in isolation.

Enlargement of the distal ends of the femur and humerus and its association with an enlarged proximal femur and proximal humerus have not been previously noted. It is unclear whether this represents a skeletal dysplasia affecting the metaphysis or whether the intervening diaphysis is disproportionately narrowed. An unusual elongation and overgrowth of the greater trochanter, present in 23% (9/39) of our cohort, also has not been previously described and might be associated with the coxa valga and coxa magna frequently observed at the proximal femur of our patient cohort.

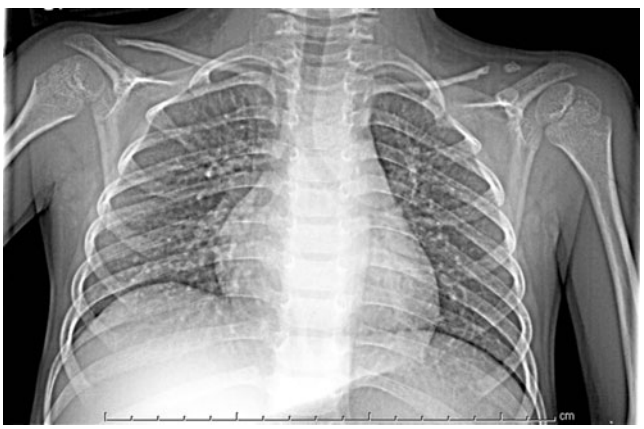

Fig. 6 Pseudoarthrosis in a 5-year-old girl with progeria. Chest radiograph shows pseudoarthrosis of the distal left clavicle. Both clavicles are thin with distal resorption

Non-traumatic (congenital) pseudoarthrosis, present in 23% (9/39) of our cohort, has rarely been reported in association with HGPS [20], although not infrequently in other multiple syndromes including fibrous dysplasia, neurofibromatosis type 1 and as an isolated phenomenon [32].

We acknowledge several study limitations. Some observations, although present, may have been affected by imaging variables. Heart size (12/39 patients: 31%) [14] and pulmonary vascular prominence (5/39 patients: 13%) were judged to be increased. However the degree of prominence was only moderate and was frequently associated with low lung volumes, which might accentuate these subjective assessments. More precise assessment of cardiovascular status has been presented in two prior natural history studies [17, 33]. Decreased skeletal mineralization, assessed as generalized osteopenia [14], was judged as present in 15/39 children (38%). This subjective assessment was considered to be mild to moderate in 14/39 and severe in degree in only 1 child. Focally accentuated osteopenia at the proximal epiphyses of the humerus and femur [13] was judged as possibly present in 4/39 children (10%). It must be emphasized, however, that osteopenia is a subjective observation based on conventional radiographic images. More objective assessment of skeletal mineralization in a subset of 26 of these children, based on DEXA and pQCT evaluations, revealed that the bone mineral density was moderately low to low when adjusted for the equivalent height age or actual cross-sectional bone geometry but that the structural geometry of the bone was significantly abnormal. The decreased size and thickness of the bone structure contributed to the apparent appearance of low bone mass [16].

HGPS exhibits abnormalities in cells and tissues of mesodermal origin such as the vasculature, cartilage, extracellular matrices and bone, where cells not only express the disease-causing protein progerin but also exhibit a wide array of in vitro and in vivo dysfunction. Although many of the precise mechanisms culminating in pathophysiology remain poorly defined, the commonality of several of our observations raises possibilities. The clustering of abnormalities at the ends of long bones (including avascular necrosis) suggests that impairment in development at secondary centers of growth (apophyses and epiphyses) relates to vascular compromise as is known to occur in both the large and small vessels in children with HGPS [14]. The presence of dystrophic soft-tissue calcification could also be secondary to microvascular compromise leading to postinfarction calcification. The cortical defects seen at several sites might relate to abnormalities of mesodermal proliferation.

This comprehensive radiographic review of 39 children with HGPS constitutes the largest aggregate of children studied collectively and approximately 15–20% of the world's population of patients with HGPS. As such it provides insight into the spectrum of skeletal dysmorphisms associated with this disease. In addition to confirming several commonly recognized manifestations of the syndrome, it provides an appreciation of their frequency and an estimate of the incidence of radiographic characteristics not previously available. Eight previously unreported observations have been recognized, several of which occurred frequently in this population. Two previously rarely recognized observations were frequently present.

Several of the observations are more common at older ages, suggesting that at least a part of the skeletal phenotype relates to an ongoing metabolic insult or buildup of abnormal tissues. This radiographic review allows us to better understand the spectrum of skeletal dysmorphisms associated with this disease and to monitor the progression and regression of the skeletal manifestations of the disease in response to treatment.

Conclusion

This report confirms commonly recognized manifestations of progeria and provides an appreciation of their frequency. For several of the observations, incidence increased with age. Additionally, eight previously unreported observations are recognized.

Acknowledgments We are grateful to the children with progeria and their families for their participation in this study. We thank the Family Inn (Cambridge, MA) and Devon Nicole House (Boston, MA) for housing families; Susan Campbell, MS, Nancy Wolf-Jenssen, and Nancy Grossman for medical records coordination; and Kyra Johnson, Kelly Littlefield, Kiera McKendrick, Angela Kraybill, and William Fletcher for coordinator services. This project was funded by The Progeria Research Foundation (PRFCLIN2007-01 and Grant #PRFCLINTRIAL003-080109), the National Heart, Lung and Blood Institute (1RC2HL101631-01), the Dana-Farber Cancer Institute Stop&Shop Pediatric Brain Tumor Program, by a National Center for Research Resources to the Children's Hospital Boston General Clinical Research Center (MO1-RR02172), and a grant from the National Center for Research Resources, National Institutes of Health, to the Harvard Catalyst Clinical & Translational Science Center (Harvard Catalyst) (UL1 RR025758-01).

Conflict of interest and disclosure The authors declare no conflict of interest.

References

1. De Sandre-Giovannoli A, Bernard R, Cau P et al (2003) Lamin A truncation in Hutchinson-Gilford progeria. Science 300:2055
2. Eriksson M, Brown WT, Gordon LB et al (2003) Recurrent de novo point mutations in lamin A cause Hutchinson-Gilford progeria syndrome. Nature 423:293–298
3. Goldman RD, Goldman AE, Shumaker DK (2005) Nuclear lamins: building blocks of nuclear structure and function. Novartis Found Symp 264:3–16, discussion 16–21, 227–230
4. Bridger JM, Kill IR (2004) Aging of Hutchinson-Gilford progeria syndrome fibroblasts is characterised by hyperproliferation and increased apoptosis. Exp Gerontol 39:717–724
5. Goldman RD, Shumaker DK, Erdos MR et al (2004) Accumulation of mutant lamin A causes progressive changes in nuclear architecture in Hutchinson-Gilford progeria syndrome. Proc Natl Acad Sci USA 101:8963–8968
6. McClintock D, Gordon LB, Djabali K (2006) Hutchinson-Gilford progeria mutant lamin A primarily targets human vascular cells as detected by an anti-Lamin A G608G antibody. Proc Natl Acad Sci USA 103:2154–2159
7. Olive M, Harten I, Mitchell R et al (2010) Cardiovascular pathology in Hutchinson-Gilford progeria: correlation with the vascular pathology of aging. Arterioscler Thromb Vasc Biol 30:2301–2309
8. Amati F, Biancolella M, D'Apice MR et al (2004) Gene expression profiling of fibroblasts from a human progeroid disease (mandibuloacral dysplasia, MAD #248370) through cDNA microarrays. Gene Expr 12:39–47
9. Csoka AB, English SB, Simkevich CP et al (2004) Genome-scale expression profiling of Hutchinson-Gilford progeria syndrome reveals widespread transcriptional misregulation leading to mesodermal/mesenchymal defects and accelerated atherosclerosis. Aging Cell 3:235–243
10. Park WY, Hwang CI, Kang MJ et al (2001) Gene profile of replicative senescence is different from progeria or elderly donor. Biochem Biophys Res Commun 282:934–939
11. Hennekam RC (2006) Hutchinson-Gilford progeria syndrome: review of the phenotype. Am J Med Genet A 140:2603–2624
12. Kieran MW, Gordon L, Kleinman M (2007) New approaches to progeria. Pediatrics 120:834–841
13. Gordon LB, McCarten KM, Giobbie-Hurder A et al (2007) Disease progression in Hutchinson-Gilford progeria syndrome: impact on growth and development. Pediatrics 120:824–833
14. Taybi H, Lachman R (1996) Progeria. In: Radiology of syndromes, metabolic disorders, and skeletal dysplasia, 4th edn. Mosby Year-Book, St. Louis, MO, pp 401–403
15. Progeria syndrome (Hutchinson-Gilford syndrome) (2006) In: Jones K (ed) Smith's recognizable patterns of human malformation, 6th edn. W.B. Saunders Co., Philadelphia, PA, pp 146–149
16. Gordon CM, Gordon LB, Snyder BD et al (2011) Hutchinson-Gilford progeria is a skeletal dysplasia. J Bone Miner Res 26: 1670–1679
17. Merideth MA, Gordon LB, Clauss S et al (2008) Phenotype and course of Hutchinson-Gilford progeria syndrome. N Engl J Med 358:592–604
18. Rosenthal IM, Bronstein IP, Dallenback FD et al (1956) Progeria: report of a case with cepalometric roentgenograms and abnormally high concentrations of lipoproteins in serum. Pediatrics 18:565–577
19. Poznanski A (1984) Metabolic bone disease and other abnormalities of the hand. In: The hand in radiologic diagnosis. W.B. Saunders Co., Philadelphia, PA, pp 839–894
20. Margolin FR, Steinbach HL (1968) Progeria Hutchinson-Gilford syndrome. AJR 103:173–178
21. Resnick D (2002) Additional congenital or heritable anomalies and syndromes. In: Resnick D (ed) Diagnosis of bone and joint disorders, 4th edn. W.B. Saunders Co., Philadelphia, PA, pp 4561–4631
22. Taybi H, Lachman R (1996) Epiphysis: dense, sclerotic, ivory. In: Radiology of syndromes, metabolic disorders, and skeletal dysplasia, 4th edn. Mosby Year-Book, St. Louis, MO, p 1029

23. Resnick D (2002) Spinal anomalies and curvatures. In: Resnick D (ed) Diagnosis of bone and joint disorders, 4th edn. W.B. Saunders Co., Philadelphia, PA, pp 4534–4559
24. (1959) Greulich W, Pyle S (eds) Radiographic atlas of skeletal development of the hand and wrist. Stanford University Press, Stanford, CA
25. Louis D, Greene T, Poznanski A (1984) Burns, frostbite, foreign bodies and other traumatic lesions of the hand. In: Poznanski A (ed) The hand in radiologic diagnosis. W.B. Saunders Co., Philadelphia, PA, pp 708–733
26. Poznanski A (1984) Joint disorders. In: The hand in radiologic diagnosis. W.B. Saunders Co., Philadelphia, PA, pp 791–838
27. Taybi H, Lachman R (1996) Scleroderma. In: Radiology of syndromes, metabolic disorders, and skeletal dysplasia, 4th edn. Mosby Year-Book, St. Louis, MO, pp 448–450
28. Resnick D (2002) Internal derangements of joints. In: Resnick D (ed) Diagnosis of bone and joint disorders, 4th edn. W.B. Saunders Co., Philadelphia, PA, pp 3019–3375
29. Poznanski A (1984) Normal variation and congenital anomalies of the wrist. In: The hand in radiologic diagnosis. W.B. Saunders Co., Philadelphia, PA, pp 181–208
30. Taybi H, Lachman R (1996) Ulna/ulnar ray: aplasia, hypoplasia. In: Radiology of syndromes, metabolic disorders, and skeletal dysplasia, 4th edn. Mosby Year-Book, St. Louis, MO, p 1044
31. Taybi H, Lachman R (1996) Madelung deformity. In: Radiology of syndromes, metabolic disorders, and skeletal dysplasia, 4th edn. Mosby Year-Book, St. Louis, MO, p 1036
32. Taybi H, Lachman R (1996) Pseudoarthrosis. In: Radiology of syndromes, metabolic disorders, and skeletal dysplasia, 4th edn. Mosby Year-Book, St. Louis, MO, pp 1039–1040
33. Gerhard-Herman M, Smoot LB, Wake N et al (2012) Mechanisms of premature vascular aging in children with Hutchinson-Gilford progeria syndrome. Hypertension 59:92–97